Catalytic Formation of Ammonia from Molecular Dinitrogen by Use of Dinitrogen-Bridged Dimolybdenum−Dinitrogen Complexes Bearing PNP-Pincer Ligands: Remarkable Effect of Substituent at PNP-Pincer Ligand

Shogo Kuriyama,[†] Kazuya Arashiba,[†] Kazunari Nakajima,[†] Hiromasa Tanaka,[‡] Nobuaki Kamaru,[§] Kazunari Yoshizawa,*[,‡,§] and Yoshiaki Nishibayashi*[,†]

[†]Institute of Engineering Innovation, School of Engineering, The University of Tokyo, Yayoi, Bunkyo-ku, Tokyo 113-8656, Japan

[‡]Elements Strategy Initiative for Catalysts and Batteries (ESICB), Kyoto University, Nishikyo-ku, Kyoto 615-8520, Japan

[§]Institute for Materials Chemistry and Engineering and International Research Center for Molecular System, Kyushu University, Nishi-ku, Fukuoka 819-0395, Japan

S *Supporting Information*

ABSTRACT: A series of dinitrogen-bridged dimolybdenum−dinitrogen complexes bearing 4-substituted PNP-pincer ligands are synthesized by the reduction of the corresponding molybdenum trichloride complexes under 1 atm of molecular dinitrogen. In accordance with a theoretical study, the catalytic activity is enhanced by the introduction of an electron-donating group to the pyridine ring of PNP-pincer ligand, and the complex bearing 4-methoxy-substituted PNP-pincer ligands is found to work as the most effective catalyst, where 52 equiv of ammonia are produced based on the catalyst (26 equiv of ammonia based on each molybdenum atom of the catalyst), together with molecular dihydrogen as a side-product. Time profiles for the catalytic reactions indicate that the rates of the formation of ammonia and molecular dihydrogen depend on the nature of the substituent on the PNP-pincer ligand of the complexes. The formation of ammonia and molecular dihydrogen is complementary in the reaction system.
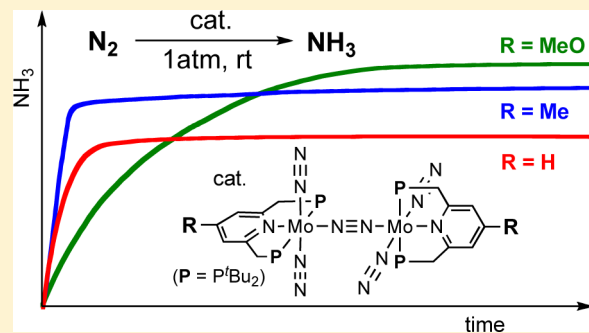
1. INTRODUCTION

Nitrogen fixation under ambient reaction conditions is one of the most important topics in chemistry. Since the finding of the first example of a transition metal−dinitrogen complex,[1] the preparation of various transition metal−dinitrogen complexes and their stoichiometric transformation of the coordinated dinitrogen have so far been well-investigated toward the end of the achievement of nitrogen fixation system under mild reaction conditions. In contrast to various studies on the stoichiometric reactivity of transition metal−dinitrogen complexes,[2,3] the catalytic transformation of molecular dinitrogen using these complexes as catalysts under mild reaction conditions is limited to only a few examples.[4]

The first successful example of the direct conversion of molecular dinitrogen into ammonia catalyzed by a transition metal−dinitrogen complex was found by Schrock and his co-worker in 2003, where a molybdenum−dinitrogen complex bearing triamidomonoamine as a tetradentate ligand worked as a catalyst to produce less than 8 equiv of ammonia based on the catalyst at ambient conditions.[5] The isolation of some reactive intermediates and DFT calculation clarified the detailed reaction pathway, what is called the Schrock cycle. More recently, we have found another successful example of the

catalytic formation of ammonia from molecular dinitrogen by using a dinitrogen-bridged dimolybdenum−dinitrogen complex bearing tridentate PNP-type pincer ligands (1a) as a catalyst, where 23 equiv of ammonia were produced based on the catalyst (12 equiv of ammonia based on each molybdenum atom of the catalyst) under ambient conditions.[6] The detailed reaction pathway remained unclear at this stage, and mononuclear molybdenum−dinitrogen complexes were considered to work as catalysts. Quite recently, Peters and co-workers have reported the third example of the conversion of molecular dinitrogen into ammonia catalyzed by iron-dinitrogen complexes bearing triphosphineborane and triphosphinealkyl ligands, where 5−7 equiv of ammonia were produced based on the catalyst at an extremely low temperature such as −78 °C.[7,8] Although the whole catalytic cycle has not yet been clarified, this is the first successful example of the iron-catalyzed direct transformation of molecular dinitrogen into ammonia under mild reaction conditions.

We have reported an experimental and theoretical study on a reaction pathway for the formation of ammonia from molecular

dinitrogen catalyzed by **1a**, where the dinuclear structure of the dinitrogen-bridged dimolybdenum–dinitrogen complex plays a decisive role in exhibiting the catalytic ability for the transformation of molecular dinitrogen into ammonia (Scheme 1).[9,10] In this reaction system, synergy between two

Scheme 1. Proposed Catalytic Cycle of Formation of Ammonia from Dinitrogen
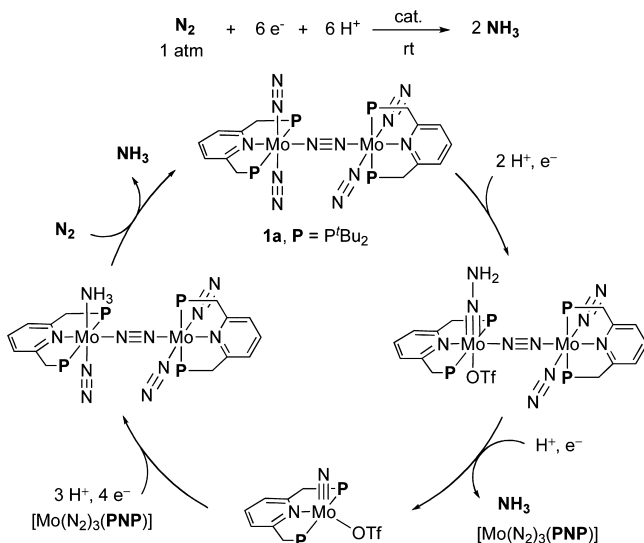

molybdenum moieties connected with a bridging dinitrogen ligand is observed at the first protonation of the coordinated dinitrogen ligand. A molybdenum core donates an electron to the active site of the other core through the bridging dinitrogen ligand, and thereby a terminal dinitrogen at the active site is reductively activated to accept a proton. This proposal indicates that a mononuclear unit of the dinuclear molybdenum-dinitrogen complex bearing PNP-type pincer ligands works as a mobile ligand to the other unit as an active site. This result is in sharp contrast to our previous proposal, where mononuclear molybdenum–dinitrogen complexes were proposed to work as key reactive intermediates.[6]

The proposed catalytic mechanism prompted us to design and prepare more reactive dinitrogen-bridged dimolybdenum–dinitrogen complexes as catalysts. On the basis of the theoretical finding that the first protonation of **1a** is considered to be one of the rate-determining steps in the catalytic cycle,[9] we have envisaged enhancing the electron-donating ability of the molybdenum center in order to accelerate the first protonation process. The introduction of an electron-donating group to the pyridine ring of **1a** is expected to intensify the back-donating ability of the molybdenum atom to the coordinated dinitrogen. In fact, the nature of substituents on the PNP-pincer ligand has substantially affected the electronic and electrochemical properties of **1**. In accordance with our design, the introduction of an electron-donating substituent such as 4-methoxy moiety into the pyridine ring of the PNP-pincer ligand has dramatically increased the catalytic activity toward the formation of ammonia. In this Article, we describe the preparation and reactivity of a series of dinitrogen-bridged dimolybdenum–dinitrogen complexes bearing 4-substituted PNP-pincer ligands. The catalytic behavior of the modified complexes is also investigated by means of experimental and theoretical methods.

2. RESULTS AND DISCUSSION

2.1. Synthesis and Properties of Dinitrogen-Bridged Dimolybdenum–Dinitrogen Complexes. A series of the dinitrogen-bridged dimolybdenum–dinitrogen complexes bearing 4-substituted PNP-pincer ligands were newly prepared according to the previous method. Treatment of [MoCl₃(4-R-PNP)] (**2**; 4-R-PNP = 4-substituted 2,6-bis(di-*tert*-butylphosphinomethyl)pyridine), which were prepared by the reaction of [MoCl₃(THF)₃] with 4-R-PNP in tetrahydrofuran (THF) at 50 °C for 18 h,[6] with 6 equiv of Na–Hg in THF at room temperature for 12 h under an atmospheric pressure of molecular dinitrogen, gave the corresponding substituted dinitrogen-bridged dimolybdenum–dinitrogen complexes [Mo-(N₂)₂(4-R-PNP)]₂(μ-N₂) (**1**) in good yields (Scheme 2).[11] A

Scheme 2. Synthesis of Dinitrogen-Bridged Dimolybdenum–Dinitrogen Complexes Bearing 4-R-PNP-Pincer Ligands (1)
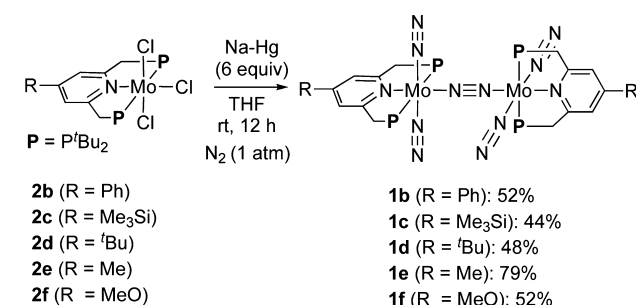
variety of substituents such as phenyl, trimethylsilyl, *tert*-butyl, methyl, and methoxy moieties could be introduced to the 4-position of the PNP-pincer ligand. These new dinitrogen-bridged dimolybdenum–dinitrogen complexes were characterized spectroscopically. Detailed molecular structures of these complexes except for **1c** were determined by X-ray crystallography. As a typical example, an ORTEP drawing of **1f** is shown in Figure 1.[12] Selected bond distances and angles
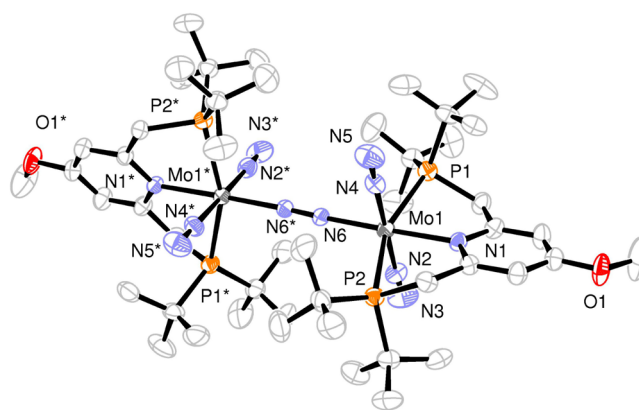

Figure 1. ORTEP drawing of **1f**. Hydrogen atoms and solvent molecules are omitted for clarity.

are shown in Supporting Information Table S8. No distinct differences were observed in the bond distances and angles of these complexes **1**. This result indicates that the introduction of a substituent at the 4-position of the pyridine ring in **1** does not significantly change the coordination environment around the molybdenum atom.

Table 1. Electronic and Electrochemical Properties of 1

complex	R	$\nu_{NN}{}^{a}$ (cm^{-1})	$E^1_{pa}{}^{b}$ (V vs Fc$^{0/+}$)	$\nu_{NN}{}^{c}$ (cm^{-1})	$q(NN_{ter})^d$
1a	H	1944	−1.67		
1b	Ph	1950	−1.64		
1c	Me$_3$Si	1947	−1.66		
1d	^{t}Bu	1939	−1.73	1960	−0.125
1e	Me	1939	−1.72	1958	−0.127
1f	MeO	1932	−1.77	1954	−0.133

^{a}All spectra were obtained in THF. ^{b}Measured by cyclic voltammetry in THF at 100 mV/s and 0.1 M of [^{n}Bu$_4$N]B(3,5-(CF$_3$)$_2$C$_6$H$_3$)$_4$. ^{c}Calculated values. ^{d}Sum of NPA charges assigned to terminal dinitrogen ligands.

In the IR spectra, the complexes **1** exhibited strong absorptions derived from the corresponding terminal dinitrogen ligands, where the nature of substituents has affected absorptions (Table 1). The presence of an electron-donating substituent at the PNP-pincer ligands in **1** caused a red-shift. For example, the dinitrogen stretching frequency of **1f** is smaller by 12 cm^{-1} than that of **1a**, indicating that the introduction of an electron-donating substituent to the pyridine ring may increase the back-donating ability of the molybdenum atom in **1** to the coordinated dinitrogen ligand.

The nature of a substituent at the PNP-pincer ligands in **1** much affected the electrochemical property of **1**. The cyclic voltammetry of **1** revealed two successive oxidation waves in the anodic scan and one reduction wave in the reverse cathodic scan (Supporting Information Figure S6 and Table S9).[13] As the electron donating ability of a substituent in **1** increased, these redox events were shifted more negatively. These redox properties of **1** are represented by first oxidation potential E^1_{pa} values in Table 1. For an example, the E^1_{pa} value of **1f** is lower than that of **1a**. A good linear relationship between the IR absorbance of the dinitrogen ligands of **1** and the oxidation potentials of **1** was observed as shown in Figure 2. These results
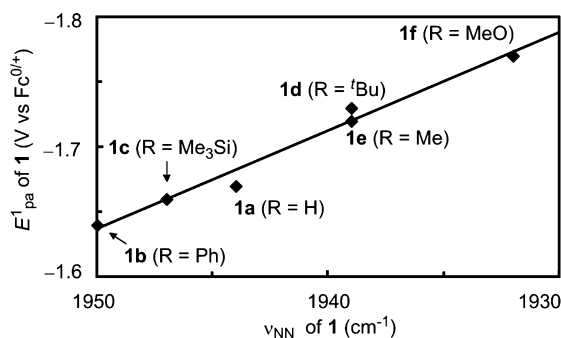

Figure 2. Relationship between dinitrogen stretching frequencies and oxidation potentials of **1** (R^2 = 0.98).

of the electronic and electrochemical properties of **1** indicate that complexes bearing a more electron-donating substituent such as **1e** and **1f** have more activated dinitrogen ligands, but the reduction steps of catalytic reactions by using **1e** and **1f** do not proceed smoothly and effectively.

2.2. DFT Calculations on the First Protonation Process. DFT calculations performed in our previous study demonstrated that the first protonation of a terminal dinitrogen ligand in **1** yielding a diazenide (−NNH) intermediate is energetically the most unfavorable process in the formation of ammonia by the use of **1** as a catalyst.[9] When 2,6-lutidinium trifluoromethanesulfonate ([LutH]OTf; Lut =2,6-lutidine; OTf = OSO$_2$CF$_3$) is adopted as a proton donor, the first

protonation process involves three elementary reaction steps as shown in Figure 3: (step A) protonation of a terminal dinitrogen ligand in **1**, (step B) elimination of the dinitrogen ligand *trans* to the generated NNH group to afford a five-coordinate diazenide intermediate, and (step C) coordination of an OTf anion to the vacant coordination site. The second and third steps should be considered as a part of the first protonation process because the first step is an endothermic reaction and thus the generated diazenide intermediate must be thermodynamically stabilized by ligand exchange of the *trans* dinitrogen ligand by OTf$^-$. In this Article, we focus on the first protonation process for the evaluation of the substituent effects in the catalytic transformation of molecular dinitrogen.

First, we have theoretically investigated energy profiles of the first protonation process in the transformation of molecular dinitrogen catalyzed by dinitrogen-bridged dimolybdenum–dinitrogen complexes bearing unsymmetrical PNP-pincer ligands. In a previous experimental work,[14] a remarkable effect of substituents at the phosphorus atom in the PNP-pincer ligand was observed: a dinitrogen-bridged dimolybdenum–dinitrogen complex bearing ^{Ad}PNP^{tBu} (^{Ad}PNP^{tBu} = 2-(di-1-adamantylphosphino)methyl-6-(di-*tert*-butylphosphino)-methylpyridine) as PNP-pincer ligand (**1h**) worked as a slightly more effective catalyst than **1a**, while a dimolybdenum–dinitrogen complex bearing ^{tBu}PNP^{Ph} (^{tBu}PNP^{Ph} = 2-(di-*tert*-butylphosphino)methyl-6-(diphenylphosphino)-methylpyridine) (**1i**) did not work at all (Scheme 3). Figure 3 shows energy profiles of the first protonation process calculated for **1a**, **1h**, and **1i**. Details on optimized structures of intermediates and transition-state structures are described in the Supporting Information. For step A, the substitution of the *tert*-butyl groups by the adamantyl groups (**1h**) decreases the activation energy (E_a) of the protonation step to 6.8 kcal/mol, while the substitution by the phenyl groups (**1i**) does not change the value of E_a (8.5 kcal/mol). The energy profile for step B exhibits a significant difference between **1a** (**1h**) and **1i**. The elimination of the dinitrogen ligand *trans* to the NNH group proceeds in an exothermic way for **1a** ($\Delta E = -2.6$ kcal/mol) and **1h** ($\Delta E = -4.2$ kcal/mol), while it is an endothermic reaction for **1i** ($\Delta E = 3.3$ kcal/mol). Additionally, the activation energy for the backward reaction (**III → II**) is calculated to be only 0.1 kcal/mol in the phenyl-substituted system. The quite low activation energy calculated for the coordination of dinitrogen to **III-i** indicates that the five-coordinate diazenide complex **III-i** should immediately accept the released dinitrogen before reacting with OTf$^-$ in the reaction solution. The regeneration of **II-i** will result in the loss of the proton added at step A because the proton detachment from **II-i** is an exothermic reaction ($\Delta E = -7.7$ kcal/mol) with a very low activation energy of 0.8 kcal/mol. On the other hand, **III-a** and **III-h** are likely to have much opportunity to accept OTf$^-$
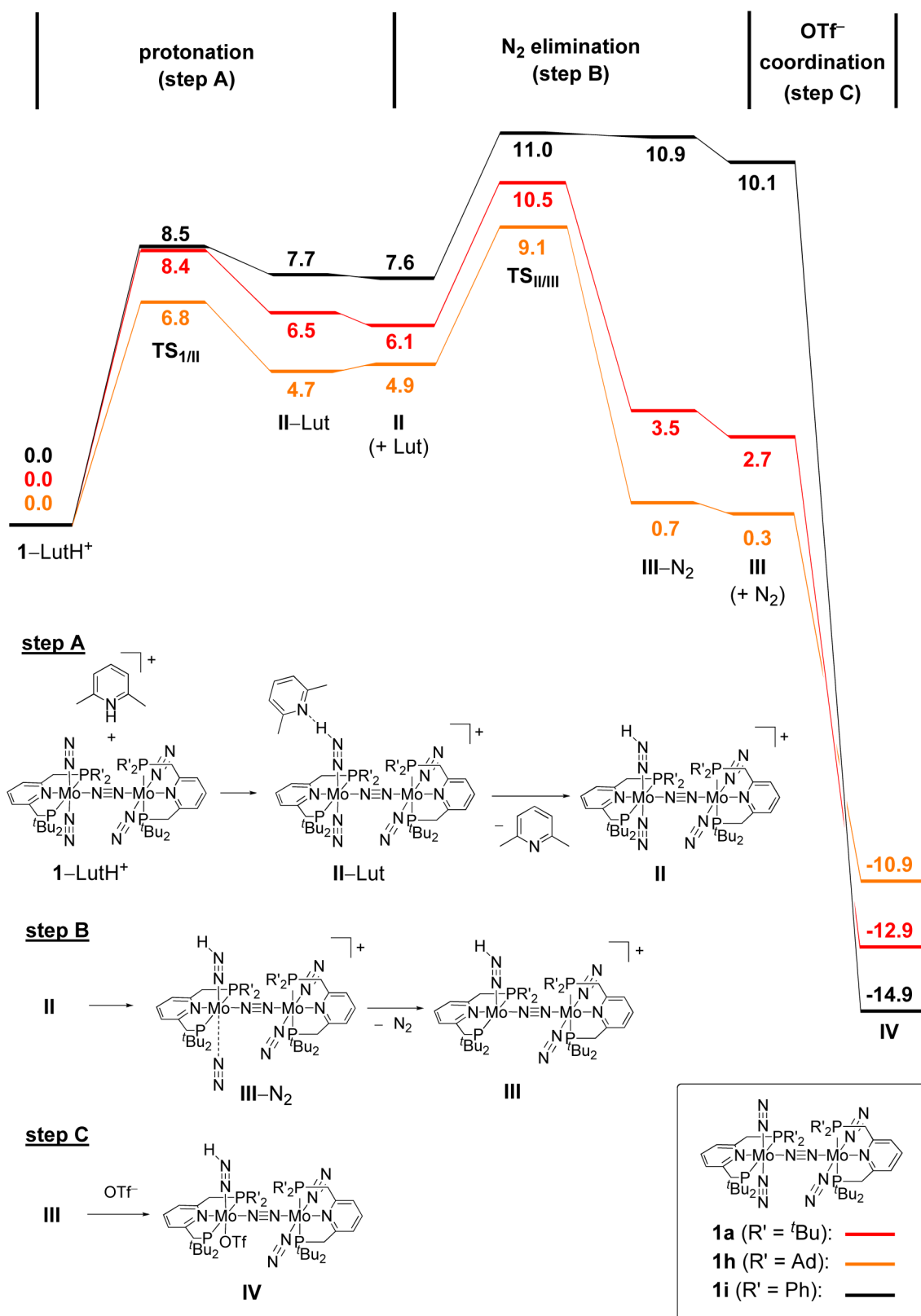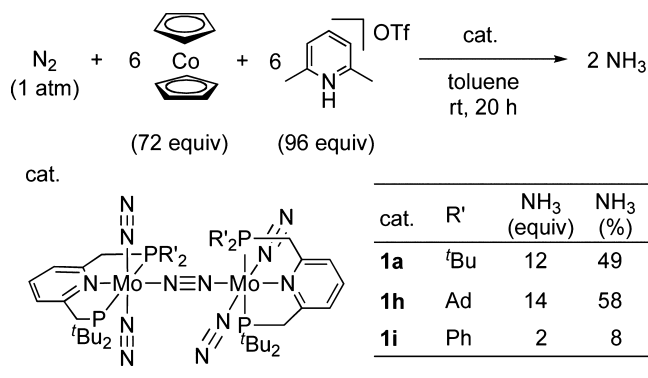
Figure 3. Energy profiles of the first protonation process of **1a**, **1h**, and **1i**. Energies relative to **1**-LutH$^+$ are presented in kcal/mol.

because of the endothermic reaction for the coordination of dinitrogen to afford **II** as well as the highly exothermic reaction for the coordination of OTf$^-$ to afford **IV** ($\Delta E = -15.6$ kcal/mol for **III-a** and -11.2 kcal/mol for **III-h**). Consequently, the lack of catalytic ability of **1i** observed in the previous work[14] can

be rationalized by the thermodynamic instability of the diazenide complexes **II-i** and **III-i**.

Next, we have theoretically examined the impact of introduction of electron-donating groups to the 4-position of the pyridine ring in the PNP-pincer ligand. Figure 4 describes

Scheme 3. Catalytic Formation of Ammonia Using Dimolybdenum–Dinitrogen Complexes Bearing Unsymmetric PNP-Pincer Ligand as Catalysts

cat.	R'	NH₃ (equiv)	NH₃ (%)
1a	^tBu	12	49
1h	Ad	14	58
1i	Ph	2	8

energy profiles of the first protonation process calculated for **1e** and **1f**, together with that of **1a**. Details on optimized structures of intermediates and transition-state structures are described in the Supporting Information. The introduction of methyl and methoxy groups to the pyridine ring does not significantly affect the trend of energy changes in the protonation process. The activation energies for the protonation of **1** are decreased to 7.4 kcal/mol for **1e** and 7.0 kcal/mol for **1f** by the introduction of an electron-donating group and those for the proton detachment from **II** are increased to 2.4 kcal/mol for **II-e** and 2.7 kcal/mol for **II-f**. The methyl and methoxy groups introduced to the pyridine ring can accelerate the protonation of **1**, although this reaction step is still endothermic. Table 1 summarizes the calculated N≡N stretching frequency and the sum of atomic charges assigned to terminal dinitrogen ligands in **1a**, **1e**, and **1f**. The atomic charges were obtained with the natural population analysis (NPA).[15] The N≡N stretching frequency calculated for **1a** (1960 cm⁻¹) is slightly red-shifted by introducing the methyl group (**1e**, 1958 cm⁻¹) and the methoxy group (**1f**, 1954 cm⁻¹), which reasonably agrees with the experimentally observed trend in Table 1. The sum of the NPA charges on dinitrogen is slightly increased by the introduction of an electron-donating group (−0.125 (**1a**) → −0.127 (**1e**) → −0.133 (**1f**)). The red-shifted N≡N stretching frequency and the increased negative NPA charge on dinitrogen indicate reductive activation of the coordinated dinitrogen through an enhanced π-back-donation. The elimination of the dinitrogen ligand (step B) proceeds in an exothermic way in all the three systems, followed by an exothermic reaction of the coordination of OTf⁻ (step C). Interestingly, the methyl and methoxy-substituted PNP-pincer ligands do not influence the energetics of step B: the values of ΔE (Eₐ) in kcal/mol are calculated to be −2.6 (4.4) for **1a**, −2.6 (4.5) for **1e**, and −2.8 (4.5) for **1f**. This result implies that the substitution of the 4-position of the pyridine ring in the PNP-pincer ligand mainly contributes to the protonation step in the first protonation process. When focusing on the first protonation process, we can expect that the catalytic ability toward the formation of ammonia from molecular dinitrogen will be improved by introducing an electron-donating group to the PNP-pincer ligand and methoxy-substituted dimolybdenum complex **1f** would serve as one of the most effective catalysts for the transformation of molecular dinitrogen into ammonia.

2.3. Catalytic Formation of Ammonia from Molecular Dinitrogen. *2.3.1. Effect of Substituent in PNP-Pincer Ligand.* We carried out the catalytic reduction of molecular

dinitrogen into ammonia using **1** as catalysts, according to the following modified procedure of the previous method.[6,14] To a mixture of **1** and 2,6-lutidinium trifluoromethanesulfonate (288 equiv to **1**) as a proton source in toluene was added a solution of cobaltocene (216 equiv to **1**; CoCp₂; Cp = η⁵-C₅H₅) as a reductant in toluene via a syringe pump at room temperature over a period of 1 h, followed by stirring at room temperature for another 19 h under an atmospheric pressure of dinitrogen. After the reaction, the formation of ammonia together with the formation of molecular dihydrogen was observed, the amount of which being determined by the indophenol method[16] and GC, respectively. Typical results are shown in Table 2. The yields of ammonia and molecular dihydrogen were estimated based on cobaltocene. In all cases, we did not observe the formation of other products such as hydrazine.

In either reaction using **1b** or **1c** as a catalyst, a similar amount of ammonia was produced (Table 2, runs 2 and 3). Use of **1d** and **1e** as catalysts increased the amount of ammonia, where 28 equiv and 31 equiv of ammonia were obtained based on the catalyst (Table 2, runs 4 and 5). Further, 34 equiv of ammonia were formed based on the catalyst when **1f** was used as a catalyst (Table 2, run 6). Thus, the largest amount of ammonia was formed when the most electron-donating moiety (MeO) was introduced to the PNP-pincer ligands in **1**, showing that the electronic and electrochemical properties of the substituent at the PNP-pincer ligand directly affect the catalytic activity of **1**. Separately, we confirmed the direct conversion of molecular dinitrogen into ammonia by using ¹⁵N₂ gas in place of normal ¹⁴N₂ gas.[17]

2.3.2. Time Profiles of Catalytic Formation of Ammonia. To obtain further information on the catalytic behavior, we monitored three catalytic reactions using **1a**, **1e**, and **1f** as catalysts, respectively. Results are shown in Figure 5. The catalytic conversion of molecular dinitrogen into ammonia occurred rapidly in the presence of **1a** or **1e** as a catalyst, where the formation of ammonia was almost completed within 2 h. Turnover frequencies (TOFs) by **1a** and **1e**, which were determined as mols of ammonia produced in initial 1 h per catalyst, are 17 and 28 h⁻¹, respectively. In contrast, the formation of ammonia proceeded more slowly using **1f** as a catalyst, where a longer reaction time such as 10 h was necessary to be completed in ammonia formation. TOF by **1f** as a catalyst is 7 h⁻¹, which was lower than those of **1a** and **1e**. Results of the time profiles indicate that the catalytic behavior of **1f** is quite different from those of **1a** and **1e**.

On the basis of the result of the time profile of **1f** (Figure 5), we consider that the reaction mixture was overstocked with cobaltocene at the early stage of the catalytic reaction. The excess amount of cobaltocene may react with a proton source to form the corresponding protonated cobaltocene or molecular dihydrogen via the protonated cobaltocene.[18] To prevent the presence of an excess amount of cobaltocene at the early stage, we carried out the reaction by slower addition of a toluene solution of cobaltocene via a syringe pump over a longer period such as 5 h, followed by stirring at room temperature for another 15 h. In this case, a slightly larger amount of ammonia (36 equiv) was produced based on the catalyst (Figure 6). To confirm our proposal, we monitored the catalytic reaction over a longer period (Figure 6). As shown in Figure 6, slower addition of cobaltocene to the reaction mixture lengthened the lifetime of the catalyst **1f**, where ammonia was produced even after 10 h. Finally, 52 equiv of ammonia based on **1f** (43% yield based on the cobaltocene) were produced in a
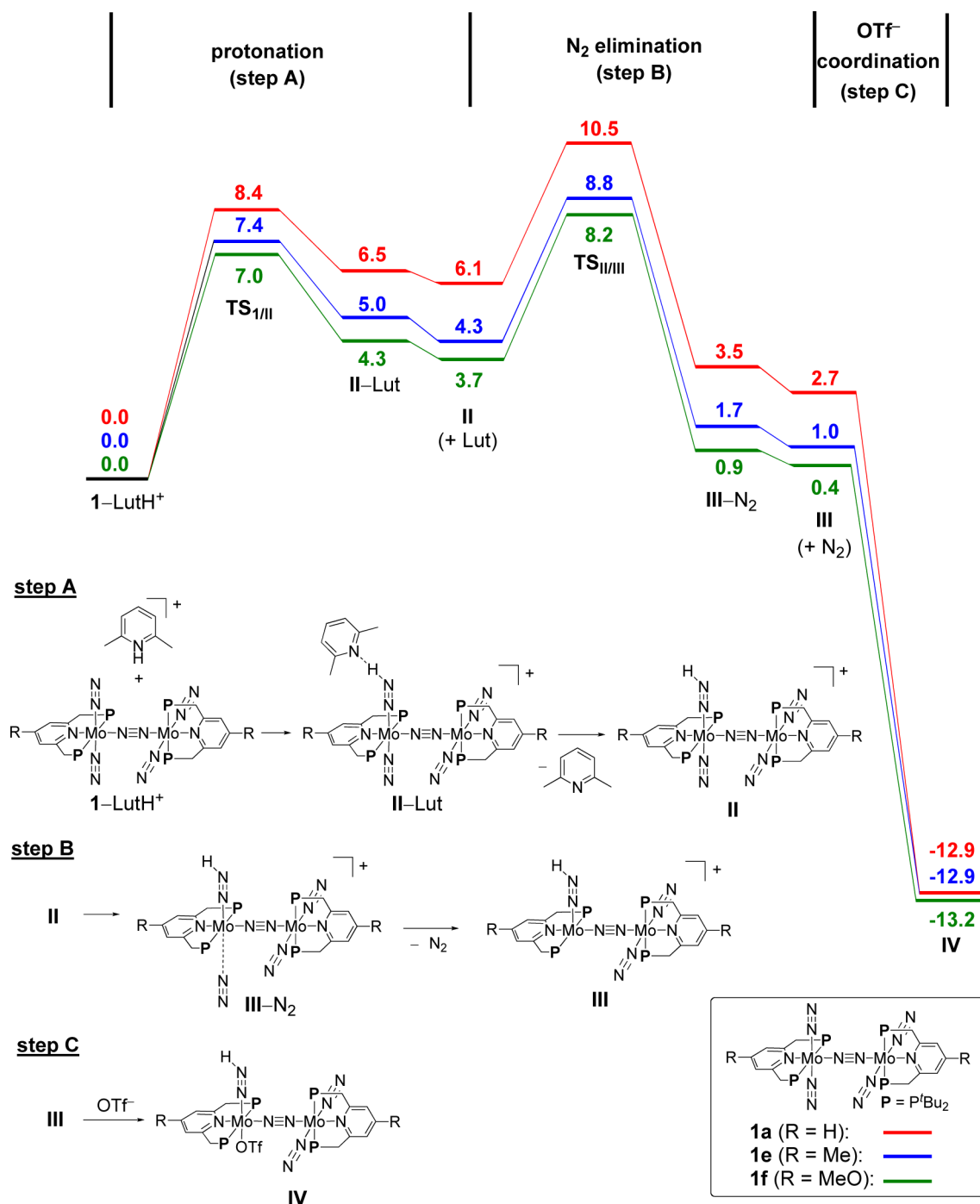
Figure 4. Energy profiles of the first protonation process of **1a**, **1e**, and **1f**. Energies relative to **1**-LutH$^+$ are presented in kcal/mol.

similar reaction using larger amounts of CoCp$_2$ (360 equiv to **1f**) and [LutH]OTf (480 equiv to **1f**). This is so far the most effective catalytic formation of ammonia from molecular dinitrogen using a transition metal−dinitrogen complex as a catalyst.

2.3.3. Effect of Reducing Reagents and Proton Sources. The reduction steps of catalytic reactions using **1e** and **1f** as catalysts did not proceed smoothly, as shown in the previous paragraphs. This result encouraged us to investigate the catalytic reaction using metallocene of a higher reducing ability such as CrCp*$_2$ (Cp* = η^5-C$_5$Me$_5$) in place of CoCp$_2$. When CrCp*$_2$ was used as a reducing reagent in the catalytic reaction in the presence of **1e** as a catalyst, almost the same amount of

ammonia were produced based on the catalysts (Table 3, run 2). In contrast to the reaction catalyzed by **1e**, only a slightly lower amount of ammonia was produced based on the catalyst when **1f** was used as a catalyst (Table 3, run 4). However, slower addition of CrCp*$_2$ to the reaction mixture increased the amount of ammonia, where up to 33 equiv of ammonia was produced based on the catalyst (Table 3, run 5). These results indicate that the use of the higher reducing reagent such as CrCp*$_2$ did not greatly affect the catalytic activity of **1e** and **1f**.

We have then investigated the effect of the acidity of a proton source on catalytic reactions by using a higher acidic proton source such as [Cl-LutH]OTf (Cl-Lut = 4-chloro-2,6-dimethylpyridine) in place of [LutH]OTf.[19] When [Cl-

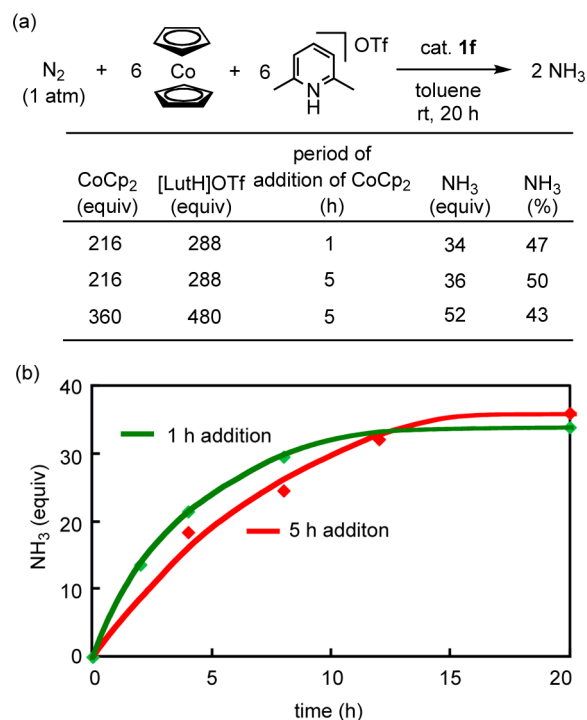**Table 2. Molybdenum-Catalyzed Reduction of Molecular Dinitrogen into Ammonia under Ambient Conditions**[a]

$$N_2 \ (1\ atm) + 6\ CoCp_2 \ (216\ equiv) + 6\ [LutH]OTf \ (288\ equiv) \xrightarrow[\substack{toluene \\ rt,\ 20\ h}]{cat.} 2\ NH_3$$

run	cat.	R	NH_3[b] (equiv)	NH_3[c] (%)	H_2 (equiv)	H_2[c] (%)
1	1a	H	23	31	46	43
2	1b	Ph	21	30	46	43
3	1c	Me₃Si	23	32	44	40
4	1d	ᵗBu	28	39	45	41
5	1e	Me	31	44	36	33
6	1f	MeO	34	47	36	33

[a]To a mixture of the catalyst (**1**: 0.010 mmol) and [LutH]OTf (288 equiv to the catalyst) as proton source in toluene (1.0 mL) was added a solution of $CoCp_2$ (216 equiv to the catalyst) as a reductant in toluene (4.0 mL) at room temperature over a period of 1 h, followed by stirring at room temperature for another 19 h under an atmospheric pressure of dinitrogen. [b]Mol equiv to the catalyst. [c]Yield based on $CoCp_2$.

$$N_2 \ (1\ atm) + 6\ CoCp_2 \ (216\ equiv) + 6\ [LutH]OTf \ (288\ equiv) \xrightarrow[\substack{toluene \\ rt}]{cat.} 2\ NH_3$$
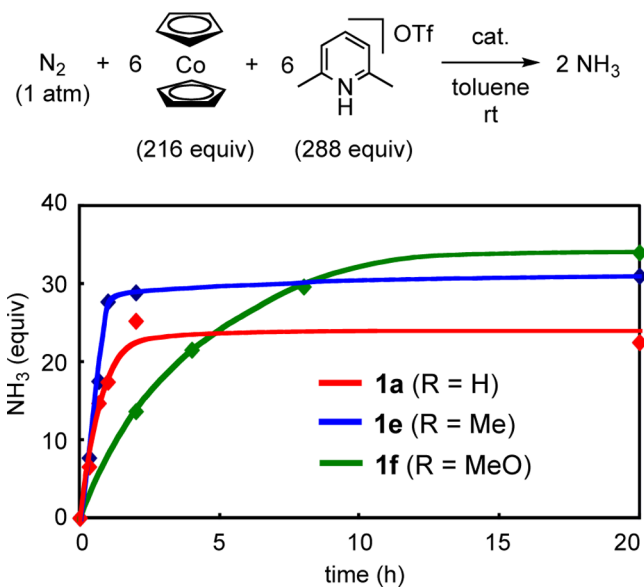
Figure 5. Time profiles of the formation of ammonia from molecular dinitrogen with **1a** (red), **1e** (blue), and **1f** (green) as catalysts.

LutH]OTf was used as a proton source in the presence of **1a** as a catalyst, only a stoichiometric amount of ammonia was produced based on the catalysts (Table 4, run 2). We consider that the protonation of cobaltocene with [Cl-LutH]OTf may proceed more smoothly because only a small amount of molecular dihydrogen was observed from the reaction mixture (see ref 18 for the acidity of the protonated cobaltocene). On the other hand, only a lower amount of ammonia (10 equiv) was produced based on the catalysts together with a larger amount of molecular dihydrogen (53 equiv) when a lower acidic proton source such as [Me-LutH]OTf (Me-Lut = 2,4,6-trimethylpyridine)[19] was used in place of [LutH]OTf in the presence of **1a** as a catalyst (Table 4, run 3). These results indicate that [LutH]OTf works as the most suitable proton source in our reaction system using **1** as catalysts.

(a)

$$N_2 \ (1\ atm) + 6\ CoCp_2 + 6\ [LutH]OTf \xrightarrow[\substack{toluene \\ rt,\ 20\ h}]{cat.\ 1f} 2\ NH_3$$

$CoCp_2$ (equiv)	[LutH]OTf (equiv)	period of addition of $CoCp_2$ (h)	NH_3 (equiv)	NH_3 (%)
216	288	1	34	47
216	288	5	36	50
360	480	5	52	43

(b)

Figure 6. (a) Catalytic formation of ammonia from molecular dinitrogen using **1f** as a catalyst. (b) Time profiles of the formation of ammonia from molecular dinitrogen with **1f** as a catalyst. A solution of $CoCp_2$ in toluene was added over a period of 1 h (green) and 5 h (red).
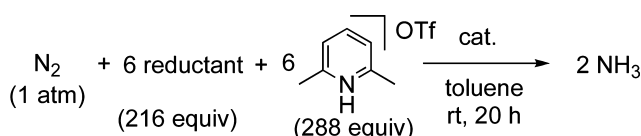
2.4. Mechanistic Investigation on Catalytic Formation of Ammonia. *2.4.1. Effect of Concentrations of Catalyst and Cobaltocene.* In the previous section, we monitored the time profiles of catalytic reactions by using three different kinds of dimolybdenum-dinitrogen complexes (**1a**, **1e**, and **1f**) as catalysts. As a result, the catalytic behavior of **1f** was revealed to be quite different from those of **1a** and **1e**. These experimental results promoted us to investigate the catalytic behavior of both **1a** and **1f** from a viewpoint of kinetic study.
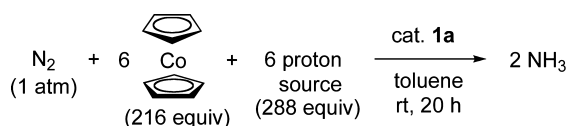
At first, we estimated the kinetic data of **1a** and **1f** for different initial concentrations of the catalyst at the early stage of catalytic reactions. The plot of the $v(NH_3)$ against the concentration of the molybdenum ([Mo]) is shown in Figure 7a. This plot shows that the $v(NH_3)$ apparently depended on [Mo] when **1a** was used as a catalyst, while $v(NH_3)$ was independent of [Mo] when **1f** was used as a catalyst. According to the plot of the $\log(v(NH_3))$ against $\log[Mo]$ shown in Figure 7b, the reaction orders with respect to the molybdenum were estimated to be ca. 1 for **1a** and 0 for **1f**, respectively. Thus, the reaction order to the molybdenum depends on the nature of catalysts. At present, we consider that both reactions using **1a** and **1f** as catalysts proceed via a similar reaction pathway, but the rate-determining steps are quite different in two reaction pathways.

Next, we estimated the kinetic data of **1a** and **1f** for different initial concentrations of cobaltocene at the early stage of catalytic reactions. The plot of $v(NH_3)$ against the concentration of cobaltocene ([CoCp_2]) is shown in Figure 8a. According to the plot of $\log(v(NH_3))$ against $\log[CoCp_2]$ shown in Figure 8b, the reaction order with respect to the cobaltocene was ca. 1 for both cases. Thus, almost the first order to the [CoCp_2] was observed in both reaction systems.

Table 3. Molybdenum-Catalyzed Reduction of Molecular Dinitrogen with [LutH]OTf and Reductant in the Presence of 1e and 1f[a]

$$N_2 \;(1\,atm) + 6\;reductant\;(216\;equiv) + 6\;[LutH]OTf\;(288\;equiv) \xrightarrow[\text{toluene, rt, 20 h}]{\text{cat.}} 2\;NH_3$$

run	cat.	R	reductant	$E_{1/2}{}^{b}$ (V)	$NH_3{}^{c}$ (equiv)	$NH_3{}^{d}$ (%)	$H_2{}^{c}$ (equiv)	$H_2{}^{d}$ (%)
1	1e	Me	CoCp$_2$	−1.33	31	44	36	33
2	1e	Me	CrCp*$_2$	−1.55	30	42	33	30
3	1f	MeO	CoCp$_2$	−1.33	34	47	36	33
4	1f	MeO	CrCp*$_2$	−1.55	24	33	39	37
5[e]	1f	MeO	CrCp*$_2$	−1.55	33	45	26	24

[a]To a mixture of the catalyst (1e or 1f, 0.010 mmol) and [LutH]OTf (288 equiv to the catalyst) in toluene (1.0 mL) was added a solution of reductant (216 equiv to the catalyst) in toluene (4.0 mL) at room temperature over a period of 1 h, followed by stirring at room temperature for another 19 h under an atmospheric pressure of dinitrogen. [b]V vs Fc$^{0/+}$. Electrochemical data ($E_{1/2}$) of the reductant was measured in THF, with [NBu$_4$]B(3,5-(CF$_3$)$_2$-C$_6$H$_3$)$_4$ as supporting electrolyte. [c]Mol equiv to the catalyst. [d]Yield based on CoCp$_2$. [e]A solution of CrCp*$_2$ in toluene was added over a period of 5 h.

Table 4. Molybdenum-Catalyzed Reduction of Molecular Dinitrogen with CoCp$_2$ and a Proton Source in the Presence of 1a[a]

$$N_2\;(1\,atm) + 6\;CoCp_2\;(216\;equiv) + 6\;proton\;source\;(288\;equiv) \xrightarrow[\text{toluene, rt, 20 h}]{\text{cat. 1a}} 2\;NH_3$$

run	proton source	$pK_a{}^{b}$	$NH_3{}^{c}$ (equiv)	$NH_3{}^{d}$ (%)	H_2 (equiv)	$H_2{}^{d}$ (%)
1	[LutH]OTf	6.96	23	31	46	43
2	[Cl-LutH]OTf	5.46	2	3	11	10
3	[Me-LutH]OTf	7.55	10	14	53	49

[a]To a mixture of 1a (0.010 mmol) and a proton source (288 equiv to the catalyst) in toluene (1.0 mL) was added a solution of CoCp$_2$ (216 equiv to the catalyst) in toluene (4.0 mL) at room temperature over a period of 1 h, followed by stirring at room temperature for another 19 h under an atmospheric pressure of dinitrogen. [b]pK$_a$ values of a proton source in H$_2$O (see ref 19). [c]Mol equiv to the catalyst. [d]Yield based on CoCp$_2$.

The rate constant for use of 1f (k_{obs}(1f)) was substantially smaller than that of 1a (k_{obs}(1a)), where the relative ratio of k_{obs}(1f)/k_{obs}(1a) was estimated to be 0.5. This result shows that the reduction step with CoCp$_2$ should be involved as one of the rate-determining steps in both reaction systems. However, the reduction step for use of 1f is considered to proceed more slowly than that of 1a, due to the higher oxidation potential of 1f than that of 1a.

2.4.2. Influence of Molecular Dihydrogen. To get more insight into the unique catalytic behavior of 1, we have investigated the influence of molecular dihydrogen on the catalytic formation of ammonia. As shown in the previous sections, molecular dihydrogen was formed as a side-product in all reaction systems. For example, the formation of 13 equiv of molecular dihydrogen (37% yield based on cobaltocene) was observed in the catalytic reaction using 1a as a catalyst, where 12 equiv of ammonia (49% yield based on cobaltocene) were produced based on the catalyst (Table 5). In the absence of 1a, the formation of only 3 equiv of molecular dihydrogen (9% yield) was observed without the formation of ammonia under similar reaction conditions. In sharp contrast, the formation of 24 equiv of molecular dihydrogen (67%) was observed under 1 atm of Ar in place of N$_2$. These results indicate that 1 worked as an effective catalyst not only toward the formation of ammonia but also toward the formation of molecular dihydrogen. At present, we consider that molecular dihydrogen should be formed via molybdenum-dihydride or -dihydrogen complexes, which may be generated by the protonation of the molybdenum atom in 1 and the sequential reduction. In fact,

we have already reported the transformation of dinitrogen-bridged dimolybdenum-tetrachloride complex into 1 and molecular dihydrogen by treatment with superhydride under 1 atm of molecular dinitrogen.[20]

To obtain more information on the catalytic ability of 1 toward the formation of molecular dihydrogen, we monitored the formation of molecular dihydrogen in three catalytic reactions using 1a, 1e, and 1f as catalysts. Typical results are shown in Figure 9. In all cases, the formation of molecular dihydrogen proceeded simultaneously with the formation of ammonia, but the rate of the formation of molecular dihydrogen depends much on the nature of substituents at PNP-pincer ligands in 1. When 1a and 1e were used as catalysts, the evolution of molecular dihydrogen proceeded rapidly, where TOFs by 1a and 1e were 23 and 19 h^{-1}, respectively. In the presence of 1f as a catalyst, the evolution of molecular dihydrogen proceeded slowly, where TOF by 1f is 5 h^{-1}. These results indicate that the introduction of an electron-donating group decreased the rate of the formation of molecular dihydrogen, where the use of 1f as a catalyst suppressed the formation of molecular dihydrogen. TOFs (NH$_3$) and TOFs (H$_2$) in catalytic reactions using 1a, 1e, and 1f as catalysts are summarized in Table 6.

Next, we discuss the influence of the formation of molecular dihydrogen on the ammonia formation in the catalytic reactions using 1a, 1e, and 1f. Yields of ammonia and molecular dihydrogen using 1a, 1e, and 1f as catalysts are summarized in Figure 10. Use of 1f as a catalyst gave not only the higher yield of ammonia but also the lower yield of molecular dihydrogen
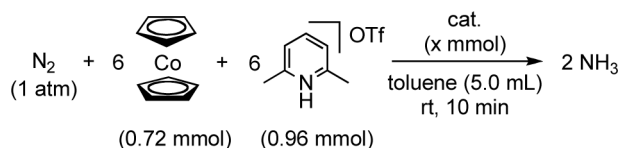
Figure 7. (a) Rate measurement for the formation of ammonia from molecular dinitrogen with **1a** (red) and **1f** (green) as catalysts at different initial Mo concentrations. (b) Plots of $\log(\nu(NH_3))$ against $\log([Mo])$.
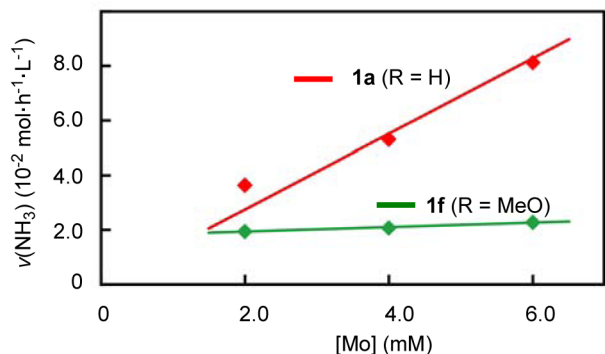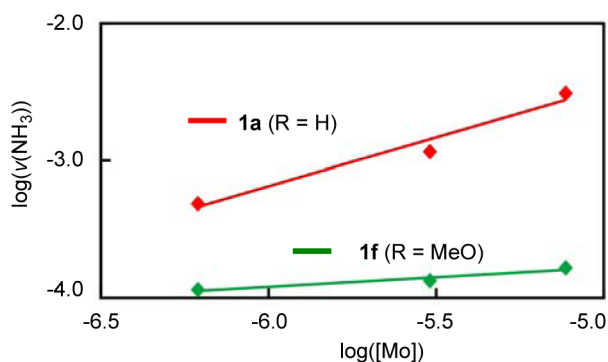

Figure 8. (a) Rate measurement for the formation of ammonia from molecular dinitrogen with **1a** (red) and **1f** (green) as catalysts at different initial $CoCp_2$ concentrations. (b) Plots of $\log(\nu(NH_3))$ against $\log([CoCp_2])$.

than those of **1a** and **1e**. These results indicate that the formation of ammonia and molecular dihydrogen is complementary in the present catalytic reaction. The formation of molecular dihydrogen should be suppressed to achieve the effective production of ammonia.

Finally, we investigated the influence of molecular dihydrogen on **1** during the catalytic reaction. Catalytic reactions using **1e** and **1f** as catalysts under 1 atm of a mixture of N_2/H_2 (96/4; 14 equiv of molecular dihydrogen based on **1** were included in a reaction flask) gave 24 equiv and 23 equiv of ammonia based on the catalysts, respectively (Table 7). In both cases, substantially lower yields of ammonia were obtained in comparison with those under 1 atm of N_2. In contrast, the reaction using **1e** as a catalyst under 1 atm of N_2 (removing the formed gases) gave a slightly higher amount of ammonia (34 equiv) based on the catalyst. On the basis of these results, we consider that molecular dihydrogen works as an inhibitor to produce ammonia in this catalytic reaction. In fact, we observed the decomposition of **1** into unidentified complexes and free PNP-pincer ligands in the reaction mixture by NMR spectroscopy when a benzene solution of **1** was exposed to molecular dihydrogen (1 atm). We consider that the ligand exchange between the coordinated dinitrogen and molecular dihydrogen may take place in the presence of a larger amount of molecular
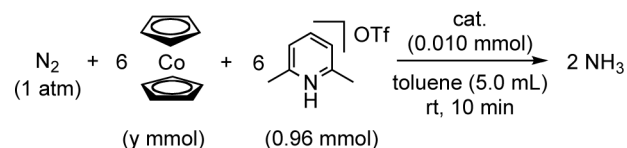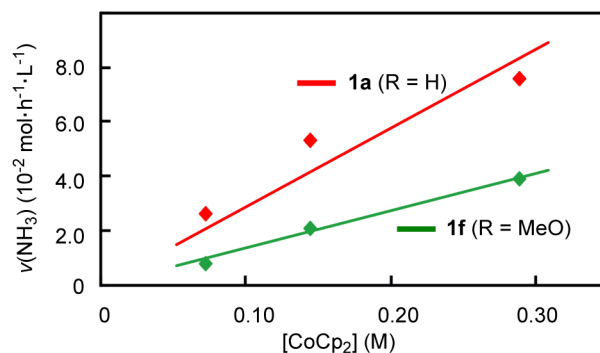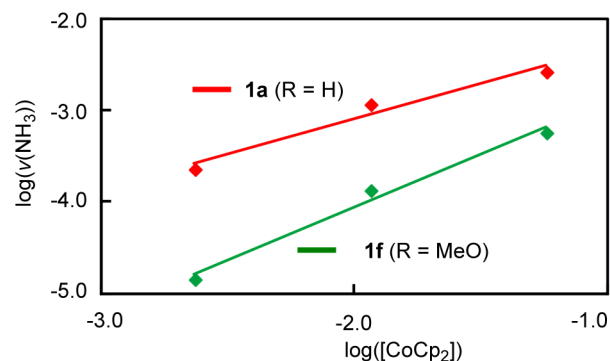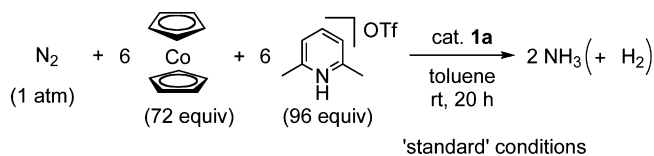
Table 5. Molybdenum-Catalyzed Reduction of Molecular Dinitrogen in the Presence of 1a under Various Reaction Conditions[a]

'standard' conditions

run	variation from the "standard" conditions	NH_3[b] (equiv)	NH_3[c] (%)	H_2[b] (equiv)	H_2[c] (%)
1	none	12	49	13	37
2	without cat. **1a**	0	0	3	9
3	Ar (1 atm) instead of N_2 (1 atm)	2	8	24	67

[a]Standard conditions: To a mixture of **1a** (0.010 mmol) and [LutH]OTf (0.96 mmol) in toluene (2.5 mL) was added a solution of $CoCp_2$ (0.72 mmol) in toluene (2.5 mL) at room temperature over a period of 5 h, followed by stirring at room temperature for another 15 h under an atmospheric pressure of dinitrogen. [b]Mol equiv to the catalyst. [c]Yield based on $CoCp_2$.

$$N_2 \;+\; 6\; \text{CoCp}_2 \;+\; 6\; [\text{LutH}]\text{OTf} \xrightarrow[\text{toluene, rt}]{\text{cat.}} 2\, NH_3 \left(+ H_2 \right)$$
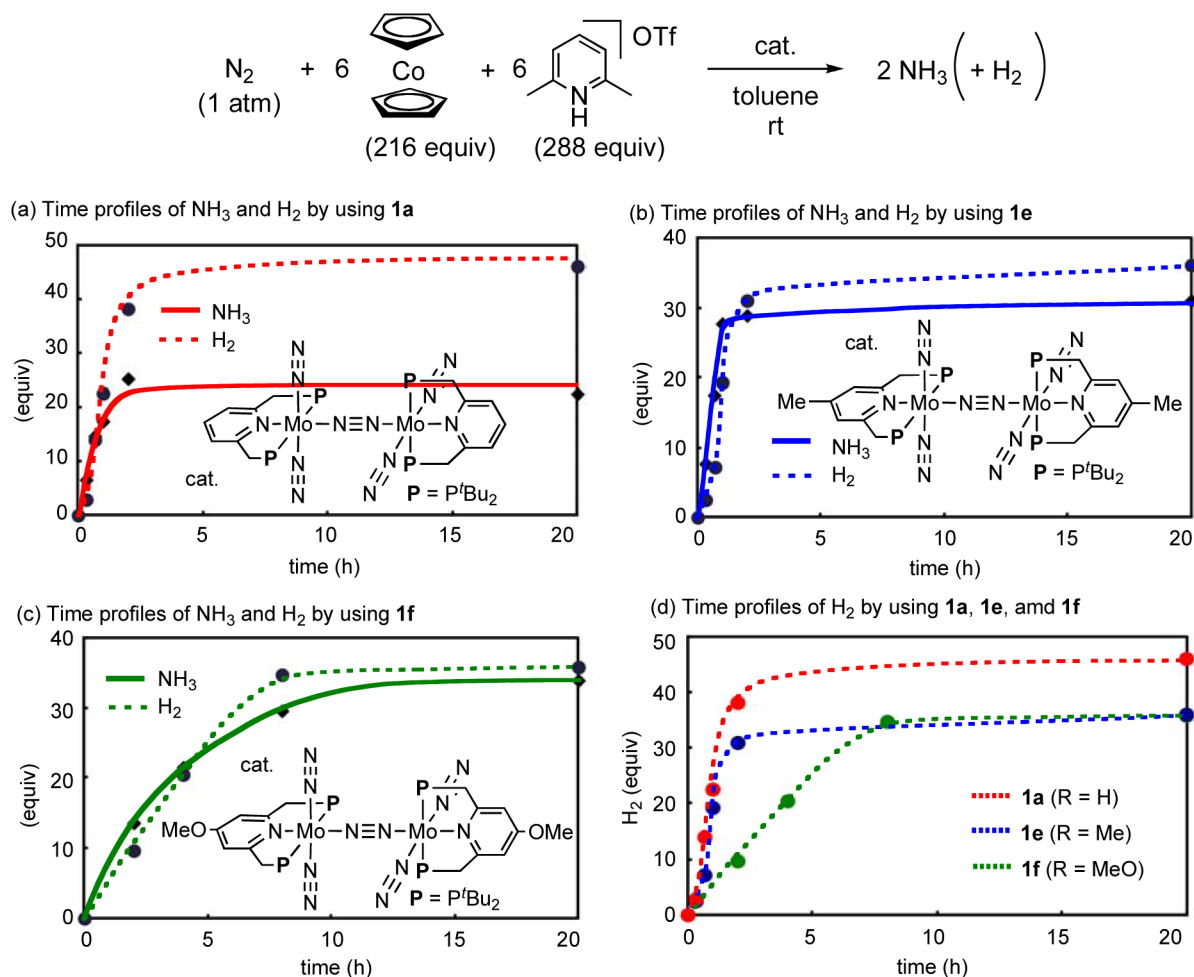

Figure 9. Time profiles of the formation of ammonia (solid line) and molecular dihydrogen (dot line) with **1a** (a), **1e** (b), and **1f** (c) as catalysts. (d) Time profiles of the formation of molecular dihydrogen with **1a**, **1e**, and **1f** as catalysts.

Table 6. TOF and TON Values for the Formation of Ammonia and Molecular Dihydrogen Catalyzed by 1a, 1e, and 1f[a]

cat.	R	TOF (NH_3) (h^{-1})	TOF (H_2) (h^{-1})	TON (NH_3)	TON (H_2)
1a	H	17	23	23	46
1e	Me	28	19	31	36
1f	MeO	7	5	34	36

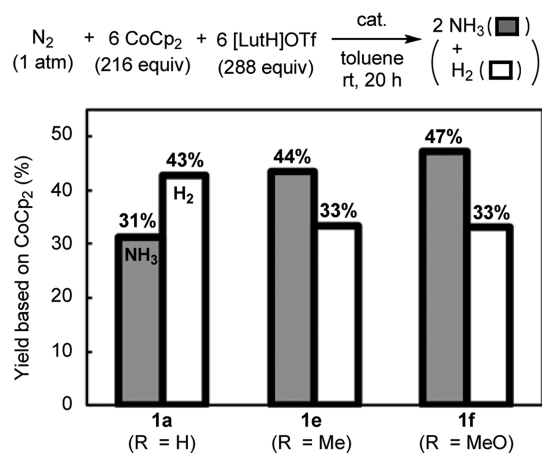[a]TOF and TON are determined based on the catalyst. See Table 2 for reaction conditions.

Figure 10. Yields of ammonia and molecular dihydrogen with **1a**, **1e**, and **1f** as catalysts.

Table 7. Molybdenum-Catalyzed Reduction of Molecular Dinitrogen in the Presence of 1e and 1f under Various Reaction Conditions[a]

run	cat.	R	gas (content)	NH_3[b] (equiv)	NH_3[c] (%)
1	**1e**	Me	N_2	31	44
2	**1f**	MeO	N_2	34	47
3	**1e**	Me	N_2/H_2 (96/4)	24	33
4	**1f**	MeO	N_2/H_2 (96/4)	23	32
5[d]	**1e**	Me	N_2	34	47

[a]See Table 2 for reaction conditions. [b]Mol equiv to the catalyst. [c]Yield based on $CoCp_2$. [d]During the catalytic reaction, formed gases were removed from the reaction flask.

dihydrogen to **1**. As the presence of molecular dihydrogen may inhibit the formation of ammonia from the catalytic reaction, the suppression of the formation of molecular dihydrogen is one of the most important factors to produce ammonia efficiently in the present reaction system.

3. CONCLUSIONS

We have newly prepared and spectroscopically characterized a series of dinitrogen-bridged dimolybdenum–dinitrogen complexes bearing a variety of 4-substituted PNP-pincer ligands. The nature of substituents at PNP-pincer ligands in the complexes substantially affects not only the electronic and electrochemical properties but also the catalytic properties toward the formation of ammonia and molecular dihydrogen. The complex bearing 4-methoxy-substituted PNP-pincer ligands **1f** has been found to work as the most effective catalyst toward the catalytic formation of ammonia from molecular dinitrogen, where 52 equiv of ammonia are produced based on the catalyst (26 equiv of ammonia based on each molybdenum atom of the catalyst). Mechanistic study indicates that the introduction of an electron-donating group to the PNP-pincer ligand accelerates the protonation steps in the first protonation process involved in the catalytic reaction. The formation of ammonia and molecular dihydrogen is complementary in the present reaction system. The suppression of the formation of molecular dihydrogen leads to achieving the effective production of ammonia. We believe that the result described in this Article provides valuable information to design a more effective catalyst toward the catalytic formation of ammonia under mild reaction conditions.[21] Further work is currently in progress to develop a more effective reaction system.

4. EXPERIMENTAL SECTION

4.1. General. ^{1}H NMR (270 MHz) and ^{31}P{^{1}H} NMR (109 MHz) spectra were recorded on a JEOL Excalibur 270 spectrometer in suitable solvents, and spectra were referenced to residual solvent (^{1}H) or external standard (^{31}P{^{1}H}: H$_3$PO$_4$). IR spectra were recorded on a JASCO FT/IR 4100 Fourier transform infrared spectrometer. Raman spectra were recorded on a JASCO NRS-2000. Absorption spectra were recorded on a Shimadzu MultiSpec-1500. Evolved dihydrogen was quantified by gas chromatography using a Shimadzu GC-8A with a TCD detector and a SHINCARBON ST (6 m × 3 mm). Elemental analyses were performed at Microanalytical Center of The University of Tokyo. Mass spectra were measured on a JEOL JMS-700 mass spectrometer. All manipulations were carried out under an atmosphere of nitrogen by using standard Schlenk techniques or glovebox techniques unless otherwise stated. Toluene was distilled from dark-blue Na/benzophenone ketyl solution and degassed, and stored over molecular sieves 4A in a nitrogen-filled glovebox. Other solvents were dried by general methods, and degassed before use. CoCp$_2$ (Aldrich) was sublimed before use. [Mo(N$_2$)$_2$(PNP)]$_2$(μ-N$_2$) (**1a**, PNP = 2,6-bis(di-t-butylphosphino)methylpyridine),[6a] [LutH]OTf,[6a] and CrCp*$_2$,[22] were prepared according to the literature methods. [Cl-LutH]OTf and [Me-LutH]OTf were prepared in a method similar to [LutH]OTf.[6a] All other reagents were commercially available.

4.2. Preparation of [Mo(N$_2$)$_2$(4-R-PNP)]$_2$(μ-N$_2$) (1). A typical procedure for the preparation of **1b**·0.5C$_6$H$_6$·0.5C$_6$H$_{14}$ is described below. To Na–Hg (0.5 wt %, 43.9 g, 10.2 mmol) were added THF (30 mL) and [MoCl$_3$(4-Ph-PNP)]·0.5CH$_2$Cl$_2$ (1.00 g. 1.40 mmol), and the mixture was stirred at room temperature for 12 h under N$_2$ (1 atm). The supernatant solution was decanted off, and the residue was washed with THF (10 mL). The combined extracts were dried *in vacuo*. After the residue was dissolved in benzene (15 mL), the solution was filtered through Celite, and the filter cake was washed with benzene three times. After the combined filtrate was concentrated to ca. 10 mL, slow addition of hexane (40 mL) afforded **1b**·0.5C$_6$H$_6$· 0.5C$_6$H$_{14}$ as brown crystals, which was collected by filtration, washed with hexane (5 mL), and dried *in vacuo* to afford **1b**·0.5C$_6$H$_6$·0.5C$_6$H$_{14}$ as a brown crystalline solid (490 mg, 0.360 mmol, 52% yield). ^{1}H NMR (C$_6$D$_6$) δ 7.53 (d, J = 7.3 Hz, Ph-*H2,6*, 4H), 7.29–7.16 (m, Ph-*H3,4,5*, 6H), 7.05 (s, Py-*H*, 4H), 3.24 (br s, C*H$_2$*P^{t}Bu$_2$, 8H), 1.44

(pseudo t, J = 5.7 Hz, CH$_2$P^{t}Bu$_2$, 72H). ^{31}P{^{1}H} NMR (C$_6$D$_6$) δ 91.1 (s). IR (KBr, cm^{-1}) 1943 (s, ν_{NN}). IR (THF, cm^{-1}) 1950 (s, ν_{NN}). Raman (THF, cm^{-1}) 1880 (ν_{NN}). Anal. Calcd for C$_{64}$H$_{104}$Mo$_2$N$_{12}$P$_4$ (**1b**·0.5C$_6$H$_6$·0.5C$_6$H$_{14}$): C, 56.63; H, 7.72; N, 12.38. Found: C, 56.92; H, 7.47; N, 11.77. The slightly low content of nitrogen is considered to be due to the labile property of the coordinated molecular dinitrogen in **1**.

4.3. [Mo(N$_2$)$_2$(4-Me$_3$Si-PNP)]$_2$(μ-N$_2$)·0.5C$_5$H$_{12}$ (1c·0.5C$_5$H$_{12}$). Recrystallization from pentane at −35 °C afforded **1c**·0.5C$_5$H$_{12}$, where a 0.5 equiv of C$_5$H$_{12}$ was determined by ^{1}H NMR. 44% yield. A green crystalline solid. ^{1}H NMR (C$_6$D$_6$) δ 7.01 (s, Py-*H*, 4H), 3.24 (br s, C*H$_2$*P^{t}Bu$_2$, 8H), 1.41 (pseudo t, J = 5.7 Hz, CH$_2$P^{t}Bu$_2$, 72H), 0.22 (s, Si*Me$_3$*, 18H). ^{31}P{^{1}H} NMR (C$_6$D$_6$) 91.5 (s). IR (KBr, cm^{-1}) 1947 (s, ν_{NN}). IR (THF, cm^{-1}) 1947 (s, ν_{NN}). Raman (THF, cm^{-1}) 1886 (ν_{NN}). Anal. Calcd for C$_{54.5}$H$_{108}$Mo$_2$N$_{12}$P$_4$Si$_2$ (**1c**·0.5C$_5$H$_{12}$): C, 50.22; H, 8.35; N, 12.89. Found: C, 49.98; H, 8.09; N, 12.34.

4.4. [Mo(N$_2$)$_2$(4-^{t}Bu-PNP)]$_2$(μ-N$_2$)·0.5C$_6$H$_{14}$ (1d·0.5C$_6$H$_{14}$). Recrystallization from hexane at −35 °C. **1d**·0.5C$_6$H$_{14}$: 48% yield. Purple crystals. ^{1}H NMR (C$_6$D$_6$) δ 6.86 (s, Py-*H*, 4H), 3.26 (br s, C*H$_2$*P^{t}Bu$_2$, 8H), 1.44 (pseudo t, J = 5.7 Hz, CH$_2$P^{t}Bu$_2$, 72H), 1.13 (s, Py-^{t}*Bu*, 18H). ^{31}P{^{1}H} NMR (C$_6$D$_6$) δ 92.3 (s). IR (KBr, cm^{-1}) 1942 (s, ν_{NN}). IR (THF, cm^{-1}) 1939 (s, ν_{NN}). Raman (THF, cm^{-1}) 1899 (ν_{NN}). Anal. Calcd for C$_{57}$H$_{109}$Mo$_2$N$_{12}$P$_4$ (**1d**·0.5C$_6$H$_{14}$): C, 53.55; H, 8.59; N, 13.15. Found: C, 53.98; H, 8.48; N, 13.20.

4.5. [Mo(N$_2$)$_2$(4-Me-PNP)]$_2$(μ-N$_2$)·C$_6$H$_{14}$ (1e·C$_6$H$_{14}$). Recrystallization from benzene−hexane afforded X-ray suitable crystals of **1e**· 2C$_6$H$_{14}$, which were collected by filtration, washed with hexane, and dried *in vacuo* to afford **1e**·C$_6$H$_{14}$ as a green crystalline solid. 79% yield. ^{1}H NMR (C$_6$D$_6$) δ 6.44 (s, Py-*H*, 4H), 3.20 (br s, C*H$_2$*P^{t}Bu$_2$, 8H), 1.82 (s, Py-*Me*, 6H), 1.44 (pseudo t, J = 5.7 Hz, CH$_2$P^{t}Bu$_2$, 72H). ^{31}P{^{1}H} NMR (C$_6$D$_6$) δ 92.3 (s). IR (KBr, cm^{-1}) 1923 (s, ν_{NN}). IR (THF, cm^{-1}) 1939 (s, ν_{NN}). Raman (THF, cm^{-1}) 1896 (ν_{NN}). Anal. Calcd for C$_{54}$H$_{104}$Mo$_2$N$_{12}$P$_4$ (**1e**·C$_6$H$_{14}$): C, 52.42; H, 8.47; N, 13.58. Found: C, 52.90; H, 8.07; N, 12.83.

4.6. [Mo(N$_2$)$_2$(4-MeO-PNP)]$_2$(μ-N$_2$)·0.5C$_6$H$_{14}$ (1f·0.5C$_6$H$_{14}$). Recrystallization from benzene−hexane afforded **1f**·0.5C$_6$H$_{14}$, where a 0.5 equiv of C$_6$H$_{14}$ was determined by ^{1}H NMR. 52% yield. A brownish purple crystalline solid. ^{1}H NMR (C$_6$D$_6$) δ 6.45 (s, Py-*H*, 4H), 3.21 (br s, C*H$_2$*P^{t}Bu$_2$, 8H), 3.18 (s, O*Me*, 6H), 1.46 (pseudo t, J = 5.7 Hz, CH$_2$P^{t}Bu$_2$, 72H). ^{31}P{^{1}H} NMR (C$_6$D$_6$) δ 92.8 (s). IR (KBr, cm^{-1}) 1924 (s, ν_{NN}). IR (THF, cm^{-1}) 1932 (s, ν_{NN}). Raman (THF, cm^{-1}) −. Analytical pure and X-ray suitable sample **1f**·C$_6$H$_{14}$ was obtained by recrystallization from toluene−hexane. Anal. Calcd for C$_{54}$H$_{104}$-Mo$_2$N$_{12}$O$_2$P$_4$ (**1f**·C$_6$H$_{14}$): C, 51.10; H, 8.26; N, 13.24. Found: C, 51.11; H, 7.58; N, 12.53.

4.7. Catalytic Reduction of Dinitrogen to Ammonia under Ambient Conditions. A typical experimental procedure for the catalytic reduction of dinitrogen into ammonia using the dinitrogen complex **1f**·0.5C$_6$H$_{14}$ is described below. In a nitrogen-filled glovebox, toluene (1.0 mL) was added to a mixture of **1f**·0.5C$_6$H$_{14}$ (12.3 mg, 0.010 mmol) and [LutH]OTf (740.9 mg, 2.88 mmol) in a 50 mL Schlenk flask. Then a solution of CoCp$_2$ (408.5 mg, 2.16 mmol) in toluene (4.0 mL) was slowly added to the stirred mixture in the Schlenk flask with a syringe pump at a rate of 4.0 mL per hour. After the addition of CoCp$_2$, the mixture was further stirred at room temperature for 19 h. The amount of dihydrogen of the catalytic reaction was determined by GC analysis. The reaction mixture was evaporated under reduced pressure, and the distillate was trapped in dilute H$_2$SO$_4$ solution (0.5 M, 10 mL). Potassium hydroxide aqueous solution (30 wt %; 5 mL) was added to the residue, and the mixture was distilled into another dilute H$_2$SO$_4$ solution (0.5 M, 10 mL). Ammonia (NH$_3$) present in each of the H$_2$SO$_4$ solutions was determined by the indophenol method.[16] The amount of ammonia was 0.043 mmol of NH$_3$ collected before base distillation of the reaction mixture and 0.296 mmol of NH$_3$ collected after base distillation to fully liberate NH$_3$, respectively. The total amount of ammonia was 0.340 mmol (34.0 equiv per **1f**).

4.8. Computational Methods. DFT calculations were performed to search all intermediates and transition structures on potential energy surfaces using the Gaussian 09 program.[23] Similar to the

previous study,[9] we adopted the B3LYP* functional, which is a reparametrized version of the B3LYP hybrid functional[24] developed by Reiher and co-workers.[25] For all intermediates calculated in the present study, the minimum-energy structures have the lowest spin multiplicity (singlet or doublet). The B3LYP and B3LYP* energy expressions are given as eq 1:

$$E_{XC}^{B3LYP} = a_0 E_X^{HF} + (1 - a_0)E_X^{LSDA} + a_x E_X^{B88} + a_c E_C^{LYP}$$
$$+ (1 - a_c)E_C^{VWN} \tag{1}$$

Here $a_0 = 0.20$ (B3LYP) or 0.15 (B3LYP*), $a_x = 0.72$, $a_c = 0.81$; also, E_X^{HF} is the Hartree–Fock exchange energy; E_X^{LSDA} is the local exchange energy from the local spin density approximation (LSDA); E_X^{B88} is Becke's gradient correction[26] to the exchange functional; E_C^{LYP} is the correlation functional developed by Lee, Yang, and Parr;[27] and E_C^{VWN} is the correlation energy calculated using the local correlation functional of Vosko, Wilk, and Nusair (VWN).[28] For optimization, the LANL2DZ and 6-31G(d) basis sets were chosen for the Mo atom and the other atoms, respectively. All stationary-point structures were found to have the appropriate number of imaginary frequencies. To determine the energy profile of the first protonation process, we performed single-point energy calculations at the optimized geometries using the Stuttgart–Dresden pseudopotentials (SDD) and 6-311+G(d,p) basis sets. Zero-point energy corrections were applied for energy changes (ΔE) and activation energies (E_a) calculated for each reaction step. Solvation effects (toluene) were taken into account by using the polarizable continuum model (PCM) in the single-point energy calculations.[29] In the calculation of the N≡N stretching frequency of **1a**, **1e**, and **1f**, solvation effects (THF) were considered by using PCM. The calculated vibrational frequencies were corrected with a scaling factor of 0.960.[30]

Protonation of a terminal dinitrogen ligand in **1** by LutH⁺ (step A) and elimination of the dinitrogen ligand trans to the NNH group (step B) were assessed from a kinetic aspect by exploring reaction pathways. Energy profiles of the coordination of OTf⁻ (step C) were calculated with a thermochemical equation, **III** + OTf⁻ → **IV**.

■ ASSOCIATED CONTENT

Ⓢ Supporting Information

Full preparative, analytical, crystallographic, and computational details. Crystallographic data in CIF format. This material is available free of charge via the Internet at http://pubs.acs.org.

■ AUTHOR INFORMATION

Corresponding Authors

kazunari@ms.ifoc.kyushu-u.ac.jp

ynishiba@sogo.t.u-tokyo.ac.jp

Notes

The authors declare no competing financial interest.

■ ACKNOWLEDGMENTS

■ REFERENCES

(1) Allen, A. D.; Senoff, C. V. *Chem. Commun.* **1965**, 621.

(2) For recent reviews, see: (a) Hinrichsen, S.; Broda, H.; Gradert, C.; Söncksen, L.; Tuczek, F. *Annu. Rep. Prog. Chem., Sect. A: Inorg. Chem.* **2012**, *108*, 17. (b) Nishibayashi, Y. *Dalton Trans.* **2012**, *41*, 7447. (c) MacLeod, K. C.; Holland, P. L. *Nat. Chem.* **2013**, *5*, 559. (d) Fryzuk, M. D. *Chem. Commun.* **2013**, *49*, 4866. (e) Broda, H.; Hinrichsen, S.; Tuczek, F. *Coord. Chem. Rev.* **2013**, *257*, 587. (f) Tanabe, Y.; Nishibayashi, Y. *Coord. Chem. Rev.* **2013**, *257*, 2551. (g) Jia, H.-P.; Quadrelli, E. *Chem. Soc. Rev.* **2014**, *43*, 547.

(3) For recent examples see: (a) Kupfer, T.; Schrock, R. R. *J. Am. Chem. Soc.* **2009**, *131*, 12829. (b) Lee, Y.; Mankad, N. P.; Peters, J. C. *Nat. Chem.* **2010**, *2*, 558. (c) Knobloch, D. J.; Lobkovsky, E.; Chirik, P. J. *Nat. Chem.* **2010**, *2*, 30. (d) Semproni, S. P.; Lobkovsky, E.; Chirik, P. J. *J. Am. Chem. Soc.* **2011**, *133*, 10406. (e) Knobloch, D. J.; Lobkovsky, E.; Chirik, P. J. *J. Am. Chem. Soc.* **2010**, *132*, 10553. (f) Rodriguez, M. M.; Bill, E.; Brennessel, W. W.; Holland, P. L. *Science* **2011**, *334*, 780. (g) Ballmann, J.; Yeo, A.; Patrick, B. O.; Fryzuk, M. D. *Angew. Chem., Int. Ed.* **2011**, *50*, 507. (h) Hebden, T. J.; Schrock, R. R.; Takase, M. K.; Müller, P. *Chem. Commun.* **2012**, *48*, 1851. (i) Semproni, S. P.; Chirik, P. J. *J. Am. Chem. Soc.* **2013**, *135*, 11373. (j) Semproni, S. P.; Chirik, P. J. *Angew. Chem., Int. Ed.* **2013**, *52*, 12965. (k) Shima, T.; Hu, S.; Luo, G.; Kang, X.; Luo, Y.; Hou, Z. *Science* **2013**, *340*, 1549. (l) Suess, D. L. M.; Peters, J. C. *J. Am. Chem. Soc.* **2013**, *135*, 4938. (m) Rittle, J.; Peters, J. C. *Proc. Natl. Acad. Sci. U.S.A.* **2013**, *110*, 15898. (n) Mock, M. T.; Chen, S.; O'Hagan, M.; Rousseau, R.; Dougherty, W. G.; Kassel, W. S.; Bullock, R. M. *J. Am. Chem. Soc.* **2013**, *135*, 11493.

(4) (a) Bazhenova, T. A.; Shilov, A. E. *Coord. Chem. Rev.* **1995**, *144*, 69. (b) Shilov, A. E. *Russ. Chem. Bull.* **2003**, *52*, 2555. (c) Shiina, K. *J. Am. Chem. Soc.* **1972**, *94*, 9266. (d) Komori, K.; Oshita, H.; Mizobe, Y.; Hidai, M. *J. Am. Chem. Soc.* **1989**, *111*, 1939. (e) Komori, K.; Sugiura, S.; Mizobe, Y.; Yamada, M.; Hidai, M. *Bull. Chem. Soc. Jpn.* **1989**, *62*, 2953. (f) Oshita, H.; Mizobe, Y.; Hidai, M. *J. Organomet. Chem.* **1993**, *456*, 213. (g) Mori, M. *J. Organomet. Chem.* **2004**, *689*, 4210. (h) Tanaka, H.; Sasada, A.; Kouno, T.; Yuki, M.; Miyake, Y.; Nakanishi, H.; Nishibayashi, Y.; Yoshizawa, K. *J. Am. Chem. Soc.* **2011**, *133*, 3498. (i) Yuki, M.; Tanaka, H.; Sasaki, K.; Miyake, Y.; Yoshizawa, K.; Nishibayashi, Y. *Nat. Commun.* **2012**, *3*, 1254.

(5) (a) Yandulov, D. V.; Schrock, R. R. *Science* **2003**, *301*, 76. (b) Ritleng, V.; Yandulov, D. V.; Weare, W. W.; Schrock, R. R.; Hock, A. S.; Davis, W. M. *J. Am. Chem. Soc.* **2004**, *126*, 6150. (c) Schrock, R. R. *Acc. Chem. Res.* **2005**, *38*, 955. (d) Weare, W. W.; Dai, X.; Byrnes, M. J.; Chin, J. M.; Schrock, R. R.; Müller, P. *Proc. Natl. Acad. Sci. U.S.A.* **2006**, *103*, 17099. (e) Schrock, R. R. *Angew. Chem., Int. Ed.* **2008**, *47*, 5512.

(6) (a) Arashiba, K.; Miyake, Y.; Nishibayashi, Y. *Nat. Chem.* **2011**, *3*, 120. (b) Arashiba, K.; Sasaki, K.; Kuriyama, S.; Miyake, Y.; Nakanishi, H.; Nishibayashi, Y. *Organometallics* **2012**, *31*, 2035.

(7) Anderson, J. S.; Rittle, J.; Peters, J. C. *Nature* **2013**, *501*, 84.

(8) Creutz, S. E.; Peters, J. C. *J. Am. Chem. Soc.* **2014**, *136*, 1105.

(9) Tanaka, H.; Arashiba, K.; Kuriyama, S.; Sasada, A.; Nakajima, K.; Yoshizawa, K.; Nishibayashi, Y. *Nat. Commun.* **2014**, *5*, 3737.

(10) Independently, Batista and coworkers have recently reported a theoretical study on our reaction pathway, where bimetallic complexes work as reactive intermediates: Tian, Y.-H.; Pierpont, A. W.; Batista, E. R. *Inorg. Chem.* **2014**, *53*, 4177.

(11) We have already tried to prepare [Mo(N₂)₂(4-Me₂N-PNP)]₂(μ-N₂) (**1g**) by a similar method. However, **1g** could not be isolated, and the reaction afforded only a mixture of unidentified complexes containing **1g**.

(12) Other ORTEP drawings are shown in the Supporting Information.

(13) Detailed electrochemical data are shown in the Supporting Information.

(14) Kinoshita, E.; Arashiba, K.; Kuriyama, S.; Miyake, Y.; Shimazaki, R.; Nakanishi, H.; Nishibayashi, Y. *Organometallics* **2012**, *31*, 8437.

(15) Glendening, E. D.; Badenhoop, J. K.; Reed, A. E.; Carpenter, J. E.; Bohmann, J. A.; Morales, C. M.; Weinhold, F. *NBO 5.9*; Theoretical Chemistry Institute, University of Wisconsin: Madison, WI, 2009; http://www.chem.wisc.edu/~nbo5.

(16) Weatherburn, M. W. *Anal. Chem.* **1967**, *39*, 971.

(17) Experimental details of $^{15}N_2$ experiment are shown in the Supporting Information.

(18) Koelle, U.; Infelta, P. P.; Grätzel, M. *Inorg. Chem.* **1988**, *27*, 879.

(19) Bips, U.; Elias, H.; Hauröder, M.; Kleinhans, G.; Pfeifer, S.; Wannowius, K. J. *Inorg. Chem.* **1983**, *22*, 3862.

(20) Arashiba, K.; Kuriyama, S.; Nakajima, K.; Nishibayashi, Y. *Chem. Commun.* **2013**, *49*, 11215.

(21) (a) Tanabe, Y.; Kuriyama, S.; Arashiba, K.; Miyake, Y.; Nakajima, K.; Nishibayashi, Y. *Chem. Commun.* **2013**, *49*, 9290. (b) Miyazaki, T.; Tanabe, Y.; Yuki, M.; Miyake, Y.; Nakajima, K.; Nishibayashi, Y. *Chem.—Eur. J.* **2013**, *19*, 11874. (c) Arashiba, K.; Nakajima, K.; Nishibayashi, Y. *Z. Anorg. Allg. Chem.* **2014**, DOI: 10.1002/zaac.201400117.

(22) Robbins, J. L.; Edelstein, N.; Spencer, B.; Smart, J. C. *J. Am. Chem. Soc.* **1982**, *104*, 1882.

(23) Frisch, M. J.; Trucks, G. W.; Schlegel, H. B.; Scuseria, G. E.; Robb, M. A.; Cheeseman, J. R.; Scalmani, G.; Barone, V.; Mennucci, B.; Petersson, G. A.; Nakat- suji, H.; Caricato, M.; Li, X.; Hratchian, H. P.; Izmaylov, A. F.; Bloino, J.; Zheng, G.; Sonnenberg, J. L.; Hada, M.; Ehara, M.; Toyota, K.; Fukuda, R.; Hasegawa, J.; Ishida, M.; Nakajima, T.; Honda, Y.; Kitao, O.; Nakai, H.; Vreven, T.; Montgomery, J. A., Jr.; Peralta, J. E.; Ogliaro, F.; Bearpark, M.; Heyd, J. J.; Brothers, E.; Kudin, K. N.; Staroverov, V. N.; Kobayashi, R.; Normand, J.; Raghavachari, K.; Rendell, A.; Burant, J. C.; Iyengar, S. S.; Tomasi, J.; Cossi, M.; Rega, N.; Millam, N. J.; Klene, M.; Knox, J. E.; Cross, J. B.; Bakken, V.; Adamo, C.; Jaramillo, J.; Gom- perts, R.; Stratmann, R. E.; Yazyev, O.; Austin, A. J.; Cammi, R.; Pomelli, C.; Ochterski, J. W.; Martin, R. L.; Morokuma, K.; Zakrzewski, V. G.; Voth, G. A.; Salvador, P.; Dannenberg, J. J.; Dapprich, S.; Daniels, A. D.; Farkas, O.; Foresman, J. B.; Ortiz, J. V.; Cioslowski, J.; Fox, D. J. *Gaussian 09, Revision B.01*; Gaussian, Inc.: Wallingford CT, 2010.

(24) (a) Becke, A. D. *J. Chem. Phys.* **1993**, *98*, 5648. (b) Stephens, P. J.; Devlin, F. J.; Chabalowski, C. F.; Frisch, M. J. *J. Phys. Chem.* **1994**, *98*, 11623.

(25) (a) Reiher, M.; Salomon, O.; Hess, B. A. *Theor. Chem. Acc.* **2001**, *107*, 48. (b) Reiher, M. *Inorg. Chem.* **2002**, *41*, 6928.

(26) Becke, A. D. *Phys. Rev. A* **1988**, *38*, 3098.

(27) Lee, C.; Yang, W.; Parr, R. G. *Phys. Rev. B* **1988**, *37*, 785.

(28) Vosko, S. H.; Wilk, L.; Nusair, M. J. *Can. J. Phys.* **1980**, *58*, 1200.

(29) Tomasi, J.; Mennucci, B.; Cammi, R. *Chem. Rev.* **2005**, *105*, 2999.

(30) Scott, A. P.; Radom, L. *J. Phys. Chem.* **1996**, *100*, 16502.